ESTIMATION OF GPS IONOSPHERIC DELAY USING L1 CODE AND CARRIER PHASE OBSERVABLES

Robert Giffard
Agilent Laboratories
3500 Deer Park Rd.
Pao Alto, CA 94304, USA

Abstract

Free electrons in the earth's ionosphere cause a frequency-dependent group delay in the bands used for the spread-spectrum GPS ranging signals. This delay constitutes a potential source of error in timing measurements. The ionospheric delay can be removed by dual-frequency ranging using the L1 and L2 signals. Two-frequency time receivers are currently expensive, and are not very reliable when tracking low elevation satellites when Anti-Spoofing is enabled, unless decryption can be used. Single-frequency, L1, receivers can correct for the delay using a detailed model of the ionosphere scaled by data contained in the 'navigation message' broadcast by the satellites. However, because of unpredictable variations of the ionosphere, this so-called single-frequency correction is only expected to absorb 50% of the effect. The uncorrected ionospheric delay can cause significant errors in L1 timing systems such as disciplined oscillators. This unpredictable source of error is of increasing importance with the approach of the solar activity maximum. Estimates of the ionospheric delay, calculated from two-frequency geodesic measurements, are now available from several sources, but these are not easy to apply in real time. In the future, WAAS and other system real-time ionosphere estimates for some geographical areas will be available with suitable receivers via geostationary satellites. We report attempts to model the zenith ionosphere correction from observations of the L1 code and carrier phase GPS observables made with a multi-channel receiver module. Code and carrier phases are affected by dispersion with opposite signs, but carrier phase always contains an ambiguity. It will be shown that by measuring derivatives of the observables, the ionospheric delay can be estimated approximately by post-processing the output of a single-frequency receiver. The use of a single frequency avoids inaccuracy due to group delay differences in the receiver for L1 and L2 signals. Real-time estimation could be performed if the batch processing procedure were replaced by a suitable filter. Preliminary results will be presented, and compared with post-processed IGS estimates.

1 INTRODUCTION

One-way time transfer using the Global Positioning System constitutes a convenient method of comparing local time scales with UTC(USNO MC). GPS-disciplined oscillators (GPSDOs) that provide an autonomous time output using this technique are now widely used. Civilian GPS users have to contend with the intentional randomization of the satellite clocks by 'Selective Availability' (SA), but if the measurements can be averaged for 1 – 2 days, the rms uncertainty is reduced to about 1 ns. We have shown elsewhere [1] that ionospheric dispersion appears to cause errors of up to 25 ns in one-way time transfer with the single-frequency receivers typically used in GPSDOs, even when the built-in ionosphere correction is used.

Worldwide estimates of the ionospheric delays are now available from the IGS and others, but these cannot be used with GPSDOs because of the computational delays of 3-7 days and the day-to-day variability of the ionosphere. It is also inconvenient if an external communication link is required at each GPSDO site. Since two-frequency time receivers that can correct for the ionosphere are not widely available, it would be very useful if a stand-alone single-frequency receiver could form a useful estimate of the local effect and correct for it in real time. Determination of the ionospheric delay by post–processing using a single-frequency receiver has previously been demonstrated [2]. Single-frequency methods of ionosphere determination avoid uncertainties associated with satellite and receiver interfrequency biases.

Report Documentation Page

Form Approved
OMB No. 0704-0188

1. REPORT DATE	2. REPORT TYPE	3. DATES COVERED
DEC 1999		**00-00-1999 to 00-00-1999**

4. TITLE AND SUBTITLE	5a. CONTRACT NUMBER
Estimation of GPS Ionospheric Delay Using L1 Code and Carrier Phase Observables	5b. GRANT NUMBER
	5c. PROGRAM ELEMENT NUMBER
6. AUTHOR(S)	5d. PROJECT NUMBER
	5e. TASK NUMBER
	5f. WORK UNIT NUMBER
7. PERFORMING ORGANIZATION NAME(S) AND ADDRESS(ES) **Agilent Laboratories,3500 Deer Park Rd,Palo Alto,CA,94304**	8. PERFORMING ORGANIZATION REPORT NUMBER
9. SPONSORING/MONITORING AGENCY NAME(S) AND ADDRESS(ES)	10. SPONSOR/MONITOR'S ACRONYM(S)
	11. SPONSOR/MONITOR'S REPORT NUMBER(S)

12. DISTRIBUTION/AVAILABILITY STATEMENT
Approved for public release; distribution unlimited

13. SUPPLEMENTARY NOTES
See also ADM001481. 31st Annual Precise Time and Time Interval (PTTI) Planning Meeting, 7-9 December 1999, Dana Point, CA

14. ABSTRACT
see report

15. SUBJECT TERMS

16. SECURITY CLASSIFICATION OF:			17. LIMITATION OF ABSTRACT	18. NUMBER OF PAGES	19a. NAME OF RESPONSIBLE PERSON
a. REPORT **unclassified**	b. ABSTRACT **unclassified**	c. THIS PAGE **unclassified**	**Same as Report (SAR)**	**13**	

In this paper, we describe experiments that have been carried out to demonstrate the estimation of the local ionospheric delay using Motorola 'ONCORE-VP' 8-channel, modular L1 time receivers. The raw data from the receivers were processed on-line by an external measurement computer in order to obtain simultaneous code range and carrier-phase data samples related to the receiver's internal clock. Estimates of the local average ionosphere delay were obtained in these experiments by subsequent off-line block-mode computation, but a real-time estimate could be obtained using suitable algorithms. The data were compared with the estimates from various processing centers through the data-base of the IGS, and agreement was found to be satisfactory. For diagnostic purposes, it was found useful to phase-lock the receiver clock oscillator to a stable external frequency reference, but this is not required in principle. It was also found useful to reduce multipath effects using a choke-ring antenna.

The model of receiver used in the experiments is now obsolete, but we feel that the technique demonstrated is general and useful, and could be used with other receivers.

2 EFFECT OF IONOSPHERE ON L1 TIME TRANSFER

The presence of free electrons in the Earth's ionosphere leads to significant dispersion at the GPS L1 and L2 frequencies [3]. The effect , in first order, is to cause the group velocity to be reduced, and the phase velocity to be increased by equal amounts. The receiver measures the range to a given satellite by code and phase tracking loops. The code tracking loop estimates the code range, ρ_{code}, given by:

$$\rho_{code} = \rho_t + c \times d_u - c \times d_s + \rho_{tropo} + \rho_{iono} + M_c. \quad (1)$$

The output of the phase-tracking loop depends on the phase range, ρ_{phase}, given by:

$$\rho_{phase} = \rho_t + c \times d_u - c \times d_s + \rho_{tropo} - \rho_{iono} + M_p. \quad (2)$$

In these equations, ρ_t is the true geometric range to the satellite, the receiver and satellite clock biases are d_u and d_s respectively, ρ_{tropo} is the path increase due to the troposphere, ρ_{iono} is the path increase equivalent to the ionospheric group delay, and c is the speed of light. The quantities M_c and M_p are code and phase errors due to multipath. The troposphere path increase is non-dispersive, and affects code and phase equally.

The theoretical path increase ρ_{iono} due to the effect of dispersion in the ionosphere is given [3] by:

$$\rho_{iono} = 40.3 \times TEC / f^2, \quad (3)$$

where TEC is the total free electron content integrated along the line of sight to the satellite in units of electrons per m^2, f is the frequency in Hz, and ρ_{iono} is in meters. TEC varies with time, and depends on the location in the ionosphere 'pierced' by the line of sight to the satellite. Equation (3) shows how the ionosphere effect depends on frequency.

At the L1 frequency, 1575.42 MHz, Equation (3) can be written for a satellite that is not at the zenith:

$$\rho_{iono} = 0.162 \times F \times TEC_v. \quad (4)$$

In Equation (4), TEC_v is the TEC value for a vertical column located at the pierce point, in units of 10^{16} electrons per m^2, and F is an obliquity factor for the line of sight to the satellite. Assuming that the active region of the ionosphere can be represented by a thin shell at an elevation of 350 km, the obliquity can be

approximately expressed [4] as a simple function of the elevation angle in degrees, E, of the satellite at the receiver's antenna:

$$F = 1 + 2.74 \times 10^{-6}(96 - E)^3. \quad (5)$$

The complex spatial and temporal variation of TEC has been extensively studied. The most obvious feature is a cyclic, daily variation. The average amplitude of the daily peak and its duration change with the season of the year, the phase of the solar cycle, and the geomagnetic latitude of the observer. There is also considerable day-to-day variability associated with solar activity. In order to estimate the ionosphere effect for one-way time transfer, both the value of TEC and the value of F averaged over the visible satellites must be known. For a receiver with a minimum elevation angle set to 15 degrees, this has been found to be about 1.8 at the latitude of the experiments to be described. Since the local TEC value can reach 75, average peak delays of 70 ns may be expected. The average delay at night falls to a minimum of about 9 ns, so that there is a strong day-night difference in the raw delay.

Conventionally, dual-frequency receivers are used to determine the ionosphere effect by observing the code ranges at the GPS L1 and L2 frequencies. Equations (1) and (3) can be used to calculate ρ_{iono} directly, or the data can be used to calculate an 'ionosphere-free' range [5]. Two-frequency receivers are significantly more complex and expensive, and the presence of the Y-code makes L2 tracking harder for non-DOD users. Compensation for the ionosphere effect determined in this way can also increase noise, and reduces the reliability of the measurements made by a stand-alone user.

The GPS system navigation message contains a correction that single-frequency receivers can use to compensate for the ionosphere effect in real time [4,6]. The correction emulates the spatial and time variation with an amplitude that is adjusted depending on observed solar radiation flux. Using the broadcast correction is expected to reduce the ionosphere effect in an L1 receiver by a factor of at least 2.0 [7].

Equations (1) and (2) suggest that the ionosphere effect might be measured by observing both the code and carrier ranges. If we calculate the code minus carrier difference, we obtain:

$$\rho_{code} - \rho_{phase} = 2 \cdot \rho_{iono} + Mc - Mp + n\lambda/2 . \quad (6)$$

In Equation (6), the term $n\lambda/2$ shows that the carrier phase measurement is ambiguous by an integer number of half wavelengths [8]. The multipath effects in the code range are generally much larger than those in phase. As long as the receiver phase-locked loops track continuously, n remains constant. Any dispersion in the receiver system will also cause unknown, but ideally constant, offsets. Because of the integer ambiguity inherent in carrier phase measurements, Equation (4) cannot be used to determine ρ_{iono} directly. During continuous phase tracking, however, it should be possible to use the time dependence of the code-carrier difference to estimate ρ_{iono}.

A complete model of the time and spatial dependence of the ionospheric dispersion given in Equation (3) is complicated. As an approximation, we will assume that the density of the ionosphere is uniform over the region sampled by the lines of sight to the satellites from the receiver, and varies with time. The simplifying assumption of local spatial uniformity should be completely acceptable in the context of time transfer because only an average of the ionosphere delay over all visible satellites is required.

Combining Equations (4) – (6), and introducing explicit time dependence, we expect the code-carrier path difference for the ith satellite, Δ_i, to vary as:

$$\Delta_i = (\rho_{code} - \rho_{phase})_i = 0.325 \times F_i(t) \times TEC_v(t) + n_i\lambda/2 + \varepsilon_i. \quad (7)$$

By differentiating Equation (7) for each of N satellites, with the assumption that there are no phase slips, we obtain the set of N equations in TEC_v, and its derivative, TEC_v':

$$\Delta_i' / 0.325 = F_1 \times TEC_v' + F_i' \times TEC_v + v_1$$

$$\ldots\ldots\ldots\ldots \quad (8)$$

$$\Delta_i' / 0.325 = F_N \times TEC_v' + F_N' \times TEC_v + v_N$$

The terms v_1 through v_N correspond to noise and errors in the derivatives of the code-carrier differences.

Since the values of F_i and the derivatives F_i' are known, the rates of change of the code-carrier differences can, in principle, be used to estimate TEC_v and its first derivative by inverting the set of Equations (8). If more than 2 satellites are tracked, a least-squares solution can be obtained using the pseudoinverse. When calculating the derivatives Δ_i' only data obtained without phase slips can be used.

3 EXPERIMENTAL DETAILS

The Motorola ONCORE-VP receiver can output serial data containing the values, at an internally defined measurement epoch, of code and carrier phase for all satellites tracked. Measurement epochs take place approximately once per second. To obtain the code-carrier differences as a function of time, it is necessary to understand the operation of the receiver in some detail.

OBTAINING RAW GPS OBSERVABLES

Signal processing in the Motorola ONCORE-VP is conerent with the receiver's crystal oscillator, which has a nominal frequency F_0 of 19,095,750 Hz. The receiver front-end down-converts the satellite carrier frequency F_c to a final baseband frequency F_b given by:

$$F_b = Fc - 82.5 \times F_0. \quad (9)$$

In Equation (9), F_c is given by:

$$F_c = 1{,}575.42 \times 10^6 + F_d. \quad (10)$$

In these equations, F_d is the Doppler frequency shift caused by motion of the satellite and the receiver. It can be seen from Equations (9) and (10) that the baseband frequency is equal to F_d plus the difference between the receiver oscillator and 19.096 MHz, multiplied by 82.5. For the nominal oscillator frequency, the baseband frequency is 20,625 + F_d Hz.

The receiver tracks the carrier phase of up to 8 satellites using software phase-locked loops. These loops operate at the baseband frequency. Each phase sample latched by the receiver at the measurement epoch is the integral from an arbitrary starting time of the frequency F_b obtained by substituting Equation (10) into Equation (9). The phase samples are reported modulo 65,536 cycles, and it is necessary to sample about once each second and keep track of rollovers.

The receiver code correlator measures the phase of the pseudo-random CA code for up to 8 satellites using software delay-locked loops operating at the baseband frequency. The output values are the phases of the code NCOs, sampled at the measurement epoch. Dithering and interpolation are used to resolve less than a single unit of NCO phase. The code phase samples are modulo 1,575,420 cycles, and data from the navigation messageareused to remove the resulting millisecond ambiguities.

The code-carrier range difference at each measurement epoch is obtained by subtracting the integral of the Doppler shift F_d multiplied by the wavelength from the code range. It appears from the frequency and time relationships discussed above that the Doppler integral has to be corrected for the integral of the baseband offset, and the code phase has to be corrected for the time delay of the epoch. However, when the code phase and the integrated Doppler shift are both expressed as ranges, these two corrections are the same. It follows that code-carrier range differences can be obtained without precise knowledge of the receiver clock frequency offset.

RECEIVER OSCILLATOR PHASE STABILIZATION

It is convenient to be able to use the continuity of the carrier-phase readings to check for phase slips. Because of the nature of the tracking loops, the smallest phase jump that can be caused by a noise transient is half a cycle, corresponding to a time of about 300 ps. To detect jumps, the rms phase run-out of the receiver clock oscillator between adjacent carrier-phase samples must therefore be much smaller than 300 ps. This corresponds to an Allan variance at 1 s of 3×10^{-10}. The free-running noise of the receiver's crystal oscillator is much larger than this.

To obtain single-satellite carrier phase data and detect phase slips, the receiver's clock offset must be stabilized. This was done in these experiments by phase-locking the receiver's TCXO to an external stable reference, an HP 5061B cesium standard. A simple 'm/n' division technique and a low-noise linear phase detector were used to lock the oscillator to a frequency of 3590/188 MHz, resulting in a baseband offset of 21,063.8297873 Hz. The loop filter has an overall loop time constant of about 0.1 second.

MEASUREMENT CO-PROCESSOR

The serial output data of the GPS receiver were fed each second to an external measurement co-processor. The signal processing program calculated the raw code and phase ranges referred to a smooth clock derived from the external oscillator. The readings were subtracted to give the code-carrier difference. Correct results required that the data from the receiver be processed each second. All the adjustments and corrections described above were carried out on-line. The resulting data were fed to digital low-pass filters, and the output for up to 8 satellites was filed on a UNIX file server each 15 seconds. The data included a UTC time-stamp and, for each satellite: PRN, elevation, azimuth, SNR, the loss-of-lock flag, and the integrated Doppler shift. The data were filed in 12-hour segments, and about 2 Mbytes of data were obtained each day in the form of ASCII files. The values of code and phase delays were propagated to integer UTC seconds using the measured Doppler frequencies.

To check the overall phase stability, raw carrier phase data were recorded each second from a chosen satellite. The average Doppler shift was obtained by subtracting successive readings, and the Doppler values were adjusted for the epoch spacing, and fed to a digital filter that tracked the average value and the first derivative with a time constant of about 5 seconds. The filter output was processed to obtain the difference between the Doppler value and the value predicted by the filter for the same time. The rms of these values was found to be approximately 0.03 cycles under ideal conditions.

Figure 1 shows a 1000-second section of Doppler residuals calculated from data recorded using the phase-locked receiver. The satellite was PRN 15, which showed no detectable SA. The data were recorded near a minimum in carrier phase, and a fifth-order fit to the time-varying Doppler shift has been subtracted in Figure 1 . The remaining deviation is due to phase noise in the receiver and the satellite signal, and quantization error in the receiver data messages. The total rms noise is 0.0053 m/s, corresponding to an L2 carrier phase error of 0.03 cycles at each measurement epoch. The phase stability corresponds to an Allan variance in frequency of about 2.0×10^{-11} at 1 second, and an rms range noise of 6 mm for phase at each sample.

Data such as that shown in Figure 1 show that the receiver, with its oscillator phase-locked to the external reference, is stable enough for the 1-second Doppler differences to be used as a check of continuous phase tracking. In fact, the receiver itself has an output signaling phase hits, and this was OR'd with the output of a discriminator on the Doppler filter in the experiments to be described. The discriminator was set to flag Doppler residuals of more than 0.4 cycles per second.

MULTIPATH ERRORS

As discussed above, the code-carrier difference is affected by multipath. This occurs because the code correlator is much more sensitive to multipath than the carrier-phase-lock loop. The ratio of sensitivity is approximately equal to the ratio of the length of a code chip in space, 300 m, to the carrier wavelength, 0.19 m. Multipath noise can be recognized by the fact that it repeats each sidereal day for a given satellite. This noise is undesirable as it reduces the accuracy of the fitting procedure expressed in Equations (8). Various antenna types were used in the course of the experiments. The final data were taken using a choke-ring antenna that seemed to reduce the multipath effects significantly. The type of antenna used is also known to have good phase center stability.

Figure 2 shows the raw code-carrier difference and the satellite elevation angle recorded during a pass of PRN 1. This pass began during the local night, when the TEC value is comparatively small, and constant. During the second half of the pass, the ionospheric delay increased to its daily maximum, causing a strongly asymmetric variation of the code-carrier difference, in contrast with the variation of the satellite elevation. The data also show a degradation of the noise level at the ends of the track due to decreasing signal strength and increasing susceptibility to multipath. The code-carrier difference is not affected by SA.

OFF-LINE DATA PROCESSING

During the experiments, data were taken continuously and processed later. This allowed various algorithms to be developed and tried on the same raw data. The data for each day were divided into 64 overlapping blocks of length 2700 s, each containing 180 15-second samples. The average rate of change of the code-carrier difference for a given satellite, within each block, was determined by a linear regression through all the points in the block. The obliquity factor for the satellite was calculated from the elevation angle using Equation (5), and a linear regression was used to determine the average and the average rate of change during the same period. The data for a given satellite were only considered valid if the loss-of-lock status flag indicated that the carrier phase was tracked continuously during the block.

For each data block, up to 8 valid sets of values of Δ_i', F_i, and F_i' could be obtained. These were then used to obtain a minimum-squares solution for TEC_v and the rate of change TEC_v' for each block using the pseudoinverse method. The uncertainty in the solution depends on the noise level on the code-carrier differences. The noise on the derivatives is reduced by extending the time over which the slope is estimated, but this cannot be too long because of the higher order time dependence of TEC_v and F_i. These considerations led to the choice of 2700 s for the block length.

The functional relationship between TEC_v and its derivative can also be used to improve the accuracy of the estimate of TEC_v. The 64 TEC_v values obtained per day were smoothed using the TEC_v' values by means of a simple recursive algorithm of the following form:

$$S_j = (1 - K)\,(S_{j-1} + \Delta t \times T_j') + K \times T_j. \qquad (11)$$

In Equation (11), S_j is the value of the estimate of TEC_v after step j, Δt is the time step, Tj' is the calculated value of TEC_v' for step j, Tj is the value of TEC_v for step j, and K is a constant smaller than 1. Values of K between 0.3 and 0.03 gave good results.

4 RESULTS AND DISCUSSION

Code-carrier data covering more than 40 days at various times during 1998 and 1999 has now been successfully recorded and analyzed using the method described above.

Figure 3 shows three days of data for the location of Agilent Laboratories, Latitude 37.4, Longitude –122.2. The two curves show the values of TEC_v and the rate of change, TEC_v', obtained by solving Equations (8). An average of about 5.5 valid data blocks was available at each point and all the data were equally weighted. The units are TEC-units and TEC-units-per-day respectively. Figure 4 shows the smoothed estimate of TEC_v obtained from the same data using the filter represented by Equation (11) with a K value of 0.1. The smoothing is obviously quite effective.

A maximum day-to-night variation of 55 TEC units is seen, corresponding to a time-transfer offset variation of 53 ns for a typical satellite constellation. The average of the TEC_v value over three days is 24, corresponding to an average uncorrected time error of 23 ns.

Several computation centers of the IGS now calculate explicit estimates of the worldwide variation of the ionospheric delay. Data from over 100 geodetic dual-frequency receivers are collected centrally and used to calculate precise satellite orbits. This orbit data are then used for post-processing in high-resolution geodesy experiments. The ionospheric delay estimates are produced as by-products of the fitting algorithms used for orbit determination. The IGS ionosphere data are available in 'IONEX' maps with a resolution of 2.5 degrees in latitude, and 5 degrees in longitude. The time step between maps is 2 hours, but accurate interpolation is possible using the fact that the ionosphere is relatively stationary in solar geocentric coordinates. The data are available 3-7 days after the observations.

In Figure 5 the single-frequency average TEC_v data obtained experimentally are compared with IGS data. The 3-day period covered is the same as that in Figure 3 . The IGS data from several sources have been used to calculate the time variation at the latitude and longitude of the experiments using the suggested interpolation procedure [9]. The single frequency data agree with the IGS data to within the scatter of the IGS data from various processing centers. The agreement with the data from the Center for Orbit Determination in Europe, Berne, is particularly good: the average and rms differences over the 3-day period are equal to –1.0 and 3.5 ns respectively.

It should be noted that the IGS products assume an ionospheric height of 450 km, which differs from the value of 350 km implicit in the use of the approximate obliquity expression, Equation (5). It is not clear at present how much this affects our results. Figure 6 shows the single-frequency data calculated over a period of 16 days between MJD 51487 and 51503. The peak TEC_v values can be seen to vary considerably over the period of a few days.

5 SUMMARY

Algorithms have been developed that allow the local vertical ionospheric delay to be determined using the GPS observables from a multi-channel, single-frequency receiver. Simultaneous measurements on several satellites are used to overcome the cycle-ambiguity of carrier-phase measurements. The algorithm assumes that the ionosphere is spatially uniform over the area sampled by the satellites. This is a relatively simple and inexpensive way of obtaining ionosphere data of moderate quality in real time. The single-frequency method is independent of receiver and satellite inter-frequency biases. Because the receiver is not required to track the L2 signal in the presence of P/Y code, the tracking is not upset by rapid scintillation or poor signal strengths at low elevations.

The TEC_v data obtained by the procedure described above have been found to lie remarkably close to the post-processed IGS estimates. The degree of agreement between these results and the IGS data for the same position seems to be between 10 and 20%. This is approximately the level to which the IGS estimates agree amongst themselves. A filter could be designed to estimate the rate of change of the code-carrier difference for each satellite tracked in real time, which would, in turn, enable the TEC_v value to be estimated in real time. This could be used with a calculated average obliquity factor to compensate the output of a time receiver directly for ionospheric delay. This should reduce the short- and long-term offsets seen [1] in one-way time transfer by a factor between 3 and 10.

The algorithms that were used to obtain these results were not optimized, and accuracy improvements could possibly be obtained by changing the block size, or by weighting the code-carrier difference data according to signal-to-noise ratio. A better understanding of the noise would also enable an optimum choice of the filter constant to be made. Further analysis of the impact of the approximations used in the processing algorithms would allow the ultimate accuracy of the method to be estimated. It would be very interesting to repeat the measurements using a receiver using narrow correlator spacing, or some other technique, to reduce the effect of multipath.

Further work should be directed to analyzing the effects of the spatial uniformity assumption and the block size on the accuracy of the TEC_v estimate. The use of a more accurate obliquity function might be helpful. It might be possible to trade some signal to noise against the introduction of spatial derivatives in the algorithm. A demonstration of the improvement in time-transfer accuracy resulting from real-time application of the autonomous TEC_v estimates should be carried out.

ACKNOWLEDGMENTS

It is a pleasure to acknowledge the encouragement of Len Cutler of Agilent Laboratories, Al Gifford of NIST, and Tom Bartholomew of TASC. Many useful interactions with Mike King of Motorola helped us to get the best out of the very versatile GPS receivers.

6 REFERENCES

[1] R.P. Giffard and R. Pitcock, "Comparison of Common-View and One-Way GPS Time Transfer Over a 4000 km East-West Baseline," presented at the 31st Annual Precise Time and Time Interval (PTTI) Systems and Applications Meeting, California, December 1999.

[2] C.E. Cohen, B. Pervan, and B.W. Parkinson, "Estimation of Absolute Ionospheric Delay Exclusively through Single-Frequency GPS Measurements," in *Proceedings of ION GPS-92*, Institute of Navigation 1992, pp. 325-330.

[3] J. A. Klobuchar, "Ionospheric effects on GPS," in *Global Positioning System: Theory and Applications,* Vol., Editors: B.W. Parkinson and J.J. Spilker, Progress in Astronautics and Aeronautics, Vol. 163, pp. 485-515.

[4] J.A. Klobuchar, "Design and Characteristics of the GPS Ionospheric Time Delay Algorithm for Single Frequency Users," in *Proceedings of the IEEE Position, Location, and Navigation Symposium*, Las Vegas, NV, USA, Nov. 1986, pp. 280-286.

[5] J.J. Spilker, "GPS Navigation Data," in *Global Positioning System: Theory and Applications*, Vol.1, Editors: B.W. Parkinson and J.J. Spilker, Progress in Astronautics and Aeronautics, Vol. 163, pp. 121-176.

[6] J.A. Klobuchar, "Present Status and Future Prospects for Ionospheric Propagation Corrections for Precise Time Transfer Using GPS," in *Proceedings of the 23rd Annual Precision Time and Time Interval (PTTI) Applications and Planning Meeting* (NASA Conference Publication 3159), 1991, pp. 417-427.

[7] *GPS Interface Control Document ICD-GPS-200*, Revision IRN-200C-002, Arinc Research Corporation, 10 Oct. 1993, pp. 124-127.

[8] A.J. Van Dierendonck, "GPS Receivers," in *Global Positioning System: Theory and Applications*, Vol.1, Editors: B.W. Parkinson and J.J. Spilker, Progress in Astronautics and Aeronautics, Vol. 163, pp. 329-407.

[9] S. Shaer and J. Feltens, "IONEX: The IONosphere Map Exchange Format Version 1," in *Proceedings of the IGS Workshop*, Darmstadt, Germany, February 1999.

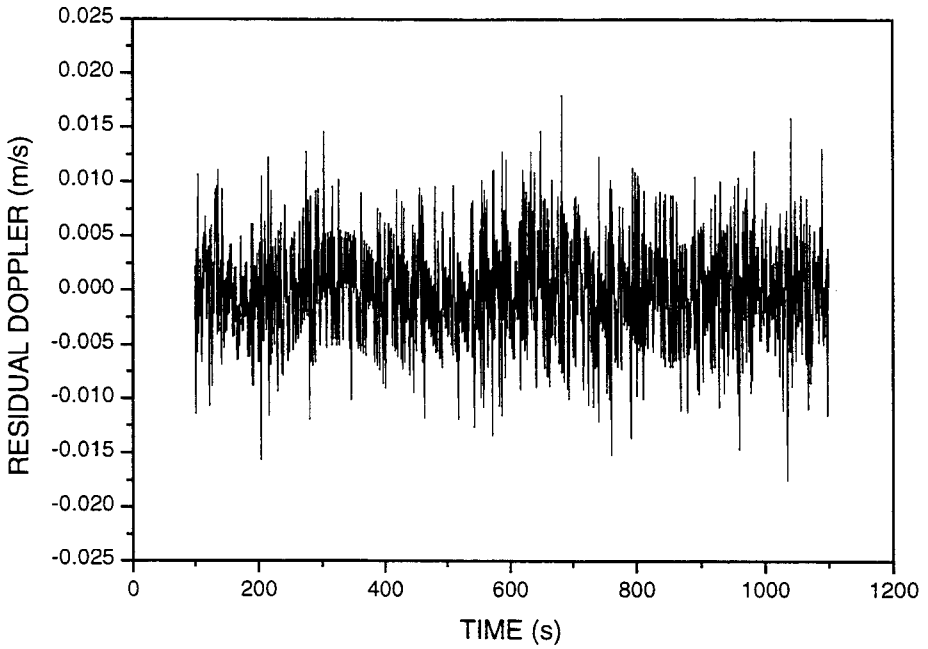

Figure 1 . Doppler shift of PRN 15 near the zenith after removal of a fifth-order polynomial fit. Measured with ONCORE-VP receiver phase-locked to HP 5061B cesium standard. PRN 15 was free of SA.

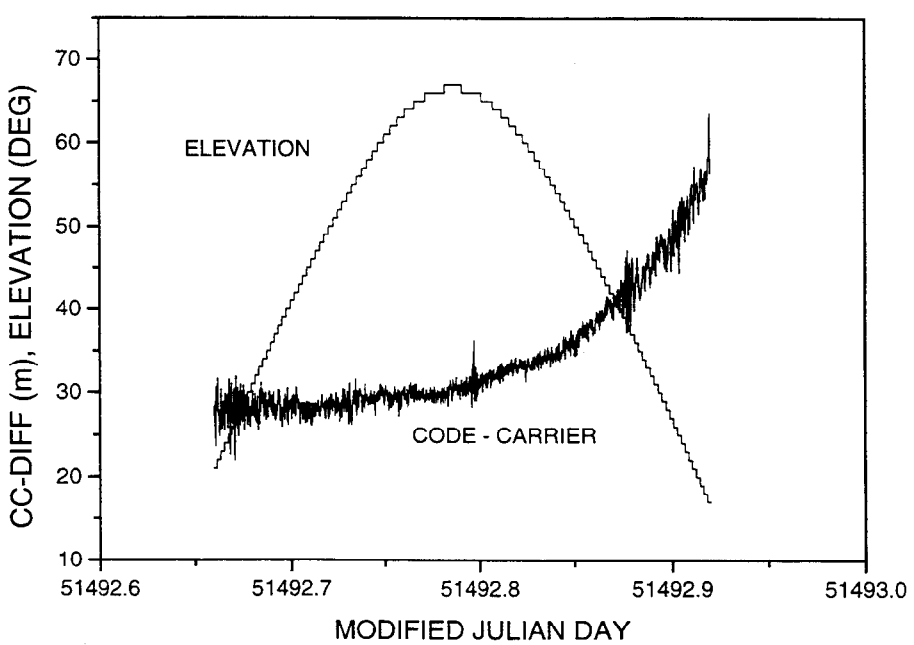

Figure 2 . The code – carrier range difference recorded during a pass of PRN 1. The satellite elevation angle is also shown. The assymetry in the variation of the code - carrier difference with elevation angle is due to the increasing ionospheric delay. The delay reaches a maximum at 14:00 local solar time or MJD 51492.92.

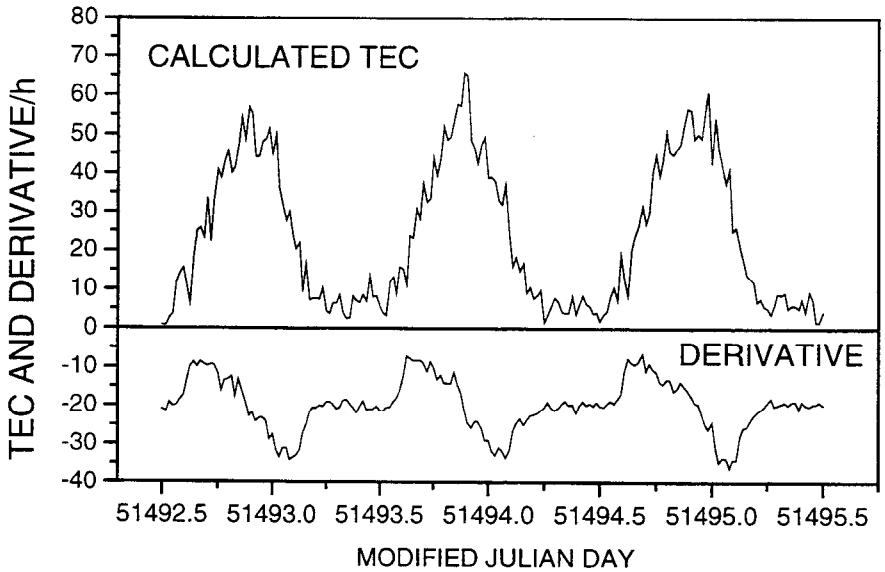

Figure 3. Values of TEC_v and the derivative TEC_v' calculated from 3 days of single-frequency measurements. The values of TEC_v' are scaled in TEC units per hour, and have been displaced –20 units for clarity.

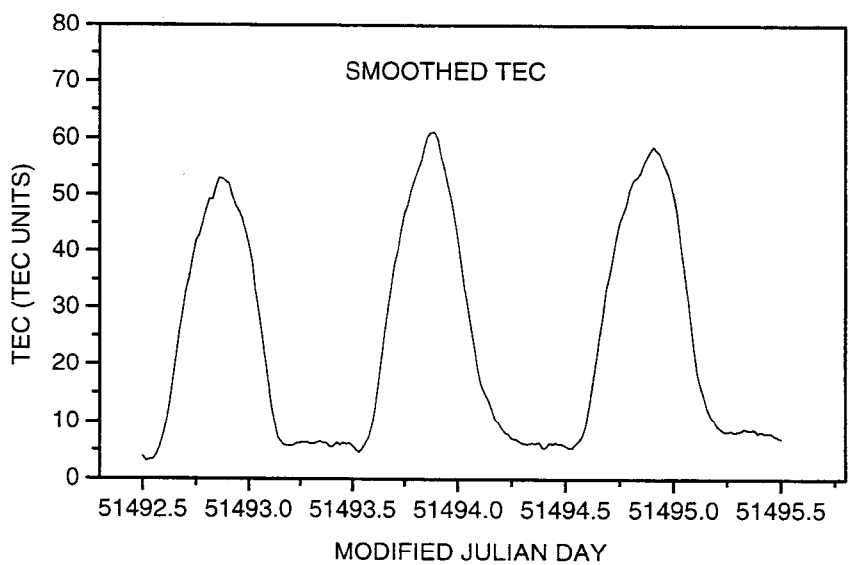

Figure 4. The smoothed estimate of the single-frequency, measured, vertical TEC calculated from the data shown in Figure (3) using Equation (11) with a K-value of 0.1. The location of the receiver is: Latitude 37.4, Longitude –122.15.

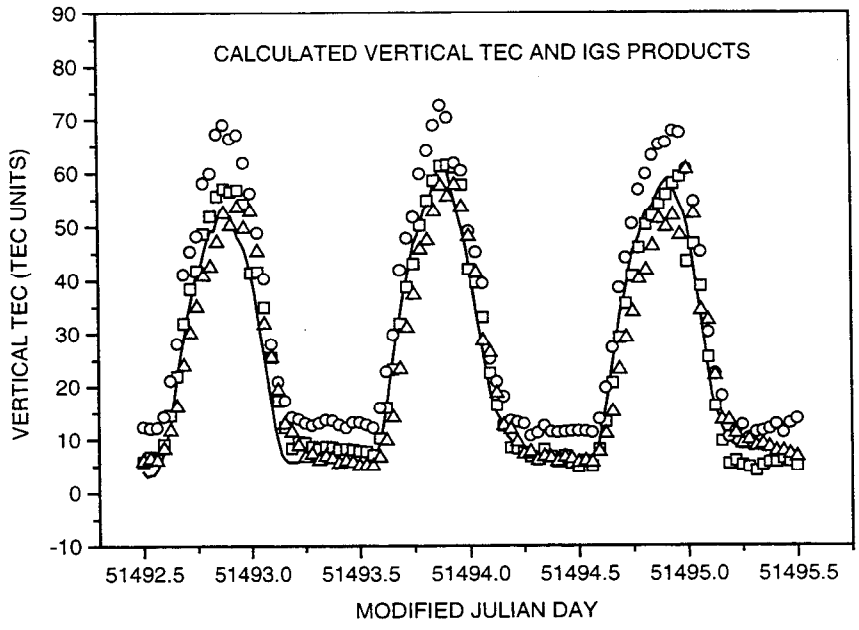

Figure 5 . The smoothed, single-frequency, local average TEC_v (solid line) calculated from the data shown in Figure 3 , compared with vertical TEC estimated for the same position constructed using IGS product data. Open squares: Center for Orbit Determination for Europe, Bern. Open circles: Jet Propulsion Laboratory, Pasadena, CA. Open triangles: National Resources, Canada.

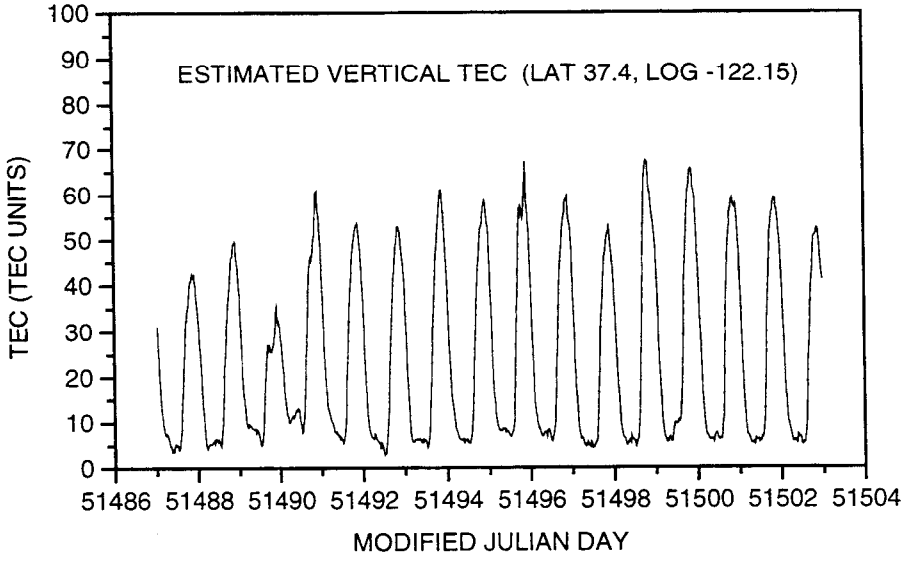

Figure 6 . Two weeks of the estimated vertical TEC in TEC-units at the location of Agilent Labs in Palo Alto, CA. The TEC is estimated from local measurements of the GPS, L1, code-carrier range difference using the algorithms described in the text.

Questions and Answers

DEMETRIOS MATSAKIS (USNO): I just want to say that we have seen at the Observatory fluctuations of up to 10 nanoseconds that we could explain by using IGS maps instead of model ionosphere. And that would bring our two frequency receivers in line with our one. I just wondered if you could turn those numbers that you have for TEC into a numerical difference?

ROBIN GIFFARD (Agilent Technologies): According to nanoseconds. Yes, it's .54 nanoseconds per TEC unit.

MATSAKIS: So, the difference between the two sites –

GIFFARD: The rms's for mine, yes, were less than a nanosecond. I'm sorry, I should have explained that.